Original article

European Journal of Microbiology and Immunology 7 (2017) 2, pp. 112–126
DOI: 10.1556/1886.2017.00007

THE GUANINE-NUCLEOTIDE EXCHANGE FACTOR CalDAG GEFI FINE-TUNES FUNCTIONAL PROPERTIES OF REGULATORY T CELLS

Jana Niemz[1], Stefanie Kliche[2], Marina C. Pils[3], Eliot Morrison[4], Annika Manns[4], Christian Freund[4], Jill R. Crittenden[5], Ann M. Graybiel[5], Melanie Galla[6], Lothar Jänsch[7], Jochen Huehn[1,*]

[1] Experimental Immunology, Helmholtz Centre for Infection Research, 38124 Braunschweig, Germany
[2] Institute of Molecular and Clinical Immunology, Health Campus Immunology, Infectiology and Inflammation, Otto-von-Guericke-University, 39120 Magdeburg, Germany
[3] Mousepathology, Helmholtz Centre for Infection Research, 38124 Braunschweig, Germany
[4] Institute for Chemistry and Biochemistry, Free University Berlin, 14195 Berlin, Germany
[5] Department of Brain and Cognitive Sciences, Massachusetts Institute of Technology, Cambridge, MA, United States
[6] Institute of Experimental Hematology, Hannover Medical School, 30625 Hannover, Germany
[7] Cellular Proteomics, Helmholtz Centre for Infection Research, 38124 Braunschweig, Germany

Received: April 7, 2017; Accepted: April 27, 2017

Using quantitative phosphopeptide sequencing of unstimulated versus stimulated primary murine Foxp3$^+$ regulatory and Foxp3$^-$ conventional T cells (Tregs and Tconv, respectively), we detected a novel and differentially regulated tyrosine phosphorylation site within the C1 domain of the guanine-nucleotide exchange factor CalDAG GEFI. We hypothesized that the Treg-specific and activation-dependent reduced phosphorylation at Y523 allows binding of CalDAG GEFI to diacylglycerol, thereby impacting the formation of a Treg-specific immunological synapse. However, diacylglycerol binding assays of phosphomutant C1 domains of CalDAG GEFI could not confirm this hypothesis. Moreover, CalDAG GEFI$^{-/-}$ mice displayed normal Treg numbers in thymus and secondary lymphoid organs, and CalDAG GEFI$^{-/-}$ Tregs showed unaltered *in vitro* suppressive capacity when compared to CalDAG GEFI$^{+/+}$ Tregs. Interestingly, when tested *in vivo*, CalDAG GEFI$^{-/-}$ Tregs displayed a slightly reduced suppressive ability in the transfer colitis model when compared to CalDAG GEFI$^{+/+}$ Tregs. Additionally, CRISPR-Cas9-generated CalDAG GEFI$^{-/-}$ Jurkat T cell clones showed reduced adhesion to ICAM-1 and fibronectin when compared to CalDAG GEFI-competent Jurkat T cells. Therefore, we speculate that deficiency in CalDAG GEFI impairs adherence of Tregs to antigen-presenting cells, thereby impeding formation of a fully functional immunological synapse, which finally results in a reduced suppressive potential.

Keywords: CalDAG GEFI, regulatory T cells, immunological synapse, adhesion, TCR signaling, phosphorylation

Introduction

T cells need activation via their T cell receptor (TCR) through interaction with a peptide-loaded major histocompatibility complex (pMHC) expressed on the surface of an antigen-presenting cell (APC) in order to exert their respective effector functions [1]. TCR stimulation is focused at the interface between T cells and APCs at the immunological synapse (IS), which is composed of the central supramolecular activation cluster (cSMAC), surrounded by a peripheral (pSMAC) and distal SMAC (dSMAC). The SMACs are primarily comprised of microclusters of TCR/CD3 molecules, integrin lymphocyte function-associated antigen-1 (LFA-1), and F-actin, respectively [2]. LFA-1 plays a dual role during T cell activation at the IS: First, interaction of LFA-1 with its ligand intercellular adhesion molecule-1 (ICAM-1) stabilizes the specific IS structure, allowing firm adhesion and stable contacts, and thereby sensitizing the TCR for very low quantities of pMHC [2–4]. Second, LFA-1 assists with integrin-mediated outside-in signaling, which serves as feedback for the T cell and delivers environmental information about chemical and

* Corresponding author: Jochen Huehn; Department Experimental Immunology, Helmholtz Centre for Infection Research, Inhoffenstraße 7, 38124 Braunschweig, Germany; Phone: +49 531 6181 3310; Fax: +49 531 6181 3399;
E-mail: Jochen.Huehn@helmholtz-hzi.de

First published online: May 22, 2017

mechanical characteristics; in this way, it supports intracellular signaling processes and also enables the deactivation and decomposition of the IS [5]. Activation of LFA-1 is facilitated in a three-step process. First, triggering of the TCR induces downstream signaling cascades, including the generation of the second messenger molecules Ca^{2+} and DAG by phospholipase γ1 (Plcγ1). This results in activation of the small GTPase Rap1, a cellular switch regulating the transition from low to intermediate affinity and clustering of LFA-1. Next, mechanical force generated through binding of LFA-1 to ICAM-1 promotes the final conversion from the intermediate- to high-affinity conformation of LFA-1 [6–8].

Rap1 activation is initiated via one of its guanine-nucleotide exchange factors, which include C3G, the CDM family member DOCK4, and Epac, PDZ-GEF or CalDAG GEF family members [9]. GEFs support the release of GDP bound by Rap1 and thereby enable binding of GTP, which activates Rap1. Functionally, Rap1 was shown to mediate extracellular regulated kinase (ERK1/2) activation and integrin-dependent cell adhesion as well as chemokine-induced migration in leukocytes [9].

The GEF CalDAG GEFI (Ca^{2+}- and DAG-regulated guanine-nucleotide exchange factor I) is mainly expressed in the central nervous system, but it can also be found in cells of hematopoietic origin, such as T cells, platelets, and neutrophils [10–13]. Guanine-nucleotide exchange activity towards Rap1 is regulated via Ca^{2+} binding to the EF hand motifs of CalDAG GEFI [10]. However, the actual responsiveness of CalDAG GEFI towards the lipid second messenger DAG via its C1 domain remains controversial [10, 14–16]. In human T cells, it was reported that CalDAG GEFI is activated upon TCR stimulation in a Plcγ1-dependent manner [11], and that it translocates to the cell membrane via interaction with polymerized actin, where it then colocalizes with Rap1 [14]. Besides TCR simulation, chemokine receptor activation such as the activation of CXCR4 via SDF-1α (CXCL12) has also been shown to trigger CalDAG GEFI in T cells [15]. Due to the specificity towards Rap1, CalDAG GEFI function also plays a role in the mechanisms of adhesion and migration. Elevated expression of CalDAG GEFI in Jurkat T cells leads to increased adhesion [11], and silencing of CalDAG GEFI in human primary T cells showed reduced adhesion following chemokine-mediated stimulation [15]. CalDAG GEFI-deficient mice have diminished Rap1 activation and display impaired adhesion and migration properties in neutrophils. However, in CalDAG GEFI-deficient platelets, Rap1 activation turned out to be delayed but robust later on, presumably owing to normal second-wave PKC-mediated activation [12, 13]. However, to the best of our knowledge, the role of CalDAG GEFI specifically in T cell subsets like regulatory T cells (Tregs) has not yet been thoroughly elucidated. Importantly, CalDAG GEFI expression has so far only been detected in human T cells and has been considered to be absent in T cells from mice [5, 12].

Tregs play a crucial role in immune homeostasis and tolerance towards self and benign antigens and are defined by the expression of the master transcription factor Foxp3 [17–21]. Disruption of the *Foxp3* locus leads to fatal autoimmunity in mice and humans, which manifests in the scurfy phenotype and immune dysregulation, polyendocrinopathy, enteropathy, and X-linked (IPEX) syndrome [22, 23]. It was already reported that the IS of Tregs and their counterparts, the conventional T cells (Tconv), differs with regard to the spatiotemporal distribution of some of the main molecular players like PKCθ [24], and that signaling downstream of TCR ligation, e.g., Ca^{2+} flux or phosphorylation of ERK, contrasts Tregs with Tconv [25–27].

The present study is based on a recently performed comparative proteome and phosphoproteome analysis of primary murine Tregs and Tconv, which not only revealed differential expression of CalDAG GEFI within these two T cell subsets, but also identified a novel phosphorylation site within CalDAG GEFI that is differentially regulated between Tregs and Tconv upon stimulation. While lipid-binding assays excluded an influence of the phosphorylation status of CalDAG GEFI on its DAG responsiveness, adhesion properties of CalDAG GEFI$^{-/-}$ Jurkat T cells were significantly impaired. Phenotyping of the T cell compartment of CalDAG GEFI$^{-/-}$ mice displayed normal T cell development and homeostasis, and CalDAG GEFI$^{-/-}$ Tregs exhibited unaltered suppressive capacity *in vitro*. However, CalDAG GEFI$^{-/-}$ Tregs showed a slightly reduced suppressive capacity *in vivo* in mice, which might be due to impaired IS formation between Tregs and APCs based on compromised LFA-1 activation.

Materials and methods

Mouse strains

BALB/c were purchased from Harlan or Janvier. CalDAG GEF$^{tm1Amg.}$ (129S4-Sv/Jae) and Rag2$^{-/-}$ (C57BL/6) mice were bred, housed and handled under specific pathogen-free conditions at the Helmholtz Centre for Infection Research (Braunschweig, Germany). Mice used in transfer colitis experiments were gender and age matched.

Antibodies and flow cytometry

Exclusion of dead cells was facilitated by LIVE/DEAD Fixable Dead Cell Stain (Invitrogen) prior to surface and intracellular staining or using propidium iodide in unfixed samples. Foxp3 staining was carried out employing Foxp3 staining kit (eBiosciences). Fluorochrome-conjugated anti-CD3 (clone 17A2), anti-CD4 (clone RM4-5), anti-CD8 (clone 53-6.7), anti-CD25 (clone PC61.5), anti-CD62L (clone MEL-14), anti-CD44 (clone IM7), anti-CD103 (clone 2E7), anti-CD152 (clone UC10-4B9), anti-Foxp3 (clone FJK-16S), anti-human CD3 (clone OKT3), anti-human CD11a (clone HI111), and anti-human CXCR4 (clone 12G5) were purchased from Biolegend or eBiosciences. Data acquisition was performed using LSRII SORP

or LSR Fortessa equipped with Diva software (BD Biosciences). Cell sorting was performed on Aria II SORP (BD Biosciences) or MoFlo XDP (Beckman Coulter). For data analysis, FlowJo software (TreeStar) was used.

Proteome and quantitative phosphopeptide sequencing

Tregs and Tconv were profiled by proteome and quantitative phosphopeptide sequencing (van Ham et al., under preparation). In brief, $CD4^+CD25^+$ Tregs and $CD4^+CD25^-$ Tconv were *ex vivo* isolated from single cell suspensions of pooled spleen and lymph node (LN) cells from BALB/c mice by MACS-based enrichment of $CD4^+$ T cells using direct beads (L3T4, Miltenyi Biotec) followed by flow cytometry-based sorting to high purity. For proteome analysis, sorted T cell subsets were left unstimulated. For quantitative phosphopeptide sequencing, cells were either left unstimulated or stimulated by decoration with biotinylated anti-CD3 (clone145-2C11, BD Biosciences) and anti-CD28 (clone 37.51, BD Biosciences) and subsequent antibody crosslinking using streptavidin. Stimulation was stopped after 5 min with an excess of ice cold PBS and cells were further processed for liquid chromatography – tandem mass spectrometry (LC–MS/MS) (further experimental details available on request).

Western blot

$CD4^+CD25^+$ Tregs and $CD4^+CD25^-$ Tconv were *ex vivo* isolated as described above. Primary T cell subsets or Jurkat T cells were lysed in RIPA lysis buffer (50 mM Tris-HCl pH 8.0, 150 mM NaCl, 0.5% sodium deoxycholate, 1% NP40, 0.1 mM PMSF, Roche Complete Mini Protease Inhibitor), and total protein concentration was determined via BCA assay following the manufacturer's instructions (Thermo Scientific). PVDF membranes were blocked using blotting-grade milk powder and specific protein bands were detected via anti-Rasgrp2 (GTX108616, Genetex), anti-β-actin (AC-74, Sigma), or anti-phosphotyrosine (4G10, Upstate) with appropriate secondary antibodies and Super Signal West Dura Extended Duration Substrate (Thermo Scientific).

Protein expression, purification, and lipid-binding assay

For expression of recombinant GST-fused C1 domain, the coding sequence of the C-terminal region of murine CalDAG GEFI (corresponding to amino acids 495-553) was amplified using forward primer 5′GAATTCATGGGCTTCGTACACAACTTC, reverse primer 5′CTCGAGCTGGGCGCGGCGACA, and Phusion Flash II DNA polymerase. The PCR product was digested with *Eco*RI/*Xho*I and subcloned into pGEX-4T-1, and the final construct was verified by sequencing. Phosphomutant C1 constructs were generated utilizing the Q5® Site-Directed Mutagenesis Kit (NEB) (Y523D: forward primer 5′CCTGGGCATCGACAAGCAGGG, reverse primer 5′ATCAGAGCTTTGCAGTGGC; Y523F: forward primer 5′CTGGGCATCTTCAAGCAGGGC, reverse primer 5′GATCAGAGCTTTGCAGTGG) according to the manufacturer's instructions. For expression, the respective plasmids were transformed into *Escherichia coli* BL21. At an optical density of 0.7–0.9 at 600 nm, 1 mM isopropylthio-β-galactoside was utilized for induction. Cells were lysed, recombinant proteins were purified via GSH columns and dialyzed against PBS or PBS supplemented with 100 µM $ZnCl_2$. Prior to lipid-binding assay, protein concentration was determined via BCA assay (Thermo Scientific), and 0.5 µg/ml of each protein was tested on membrane lipid PIP Strips (Echelon) following the manufacturer's instructions.

CRISPR-Cas9-mediated gene knock-out in Jurkat T cells

Single guide RNAs (sgRNA) targeting CalDAG GEFI in Jurkat T cells were generated utilizing the online tool http://crispr.mit.edu/ (Zhang Lab, MIT, 2015). Selected sgRNAs were cloned into pSpCas9(BB)-2A-GFP (Addgene plasmid no. 48138) via *Bbs*I restriction site; pSpCas9(BB)-2A-GFP (PX458) was a gift from Feng Zhang [28]. Jurkat T cells (JE6) were cultured in RPMI (Gibco) supplemented with 10% of fetal calf serum (FCS, Biochrom). For transfection, Jurkat T cells were electroporated employing the Amaxa Cell Line Nucleofector V Kit and the Amaxa Nucleofector device. Forty-eight hours after nucleofection, single Jurkat T cells were sorted into 96-well round bottom plates according to GFP expression. Single cell clones were expanded and tested for CalDAG GEFI expression via Western Blot.

Transduction of Jurkat T cells

To reexpress CalDAG GEFI in CalDAG $GEFI^{-/-}$ Jurkat T cell clones, lentiviral transduction was employed utilizing a modified version of pRRL-PPT-SF-IRES-EGFP-PRE [29]. To allow efficient and site-directed cloning of cDNAs upstream of the IRES sequence, a multiple cloning site (MCS) was introduced via overlapping PCR into pRRL-PPT-SF-IRES-EGFP-PRE [29]. Using the latter as a template, intermediate overlapping PCR products A and B were generated by using primer pairs MCS-For and RRL-ApaI-Rev (5′ACTAGTTC GACGCGTCAAATCTAGATTATCGATACCGGTG ACGGATCCGCCC CTCTCCCTCCCCCCCCC and 5′CAGGTTTCCGGGCCCTCACATTGCCAAA) as well as MCS-Rev and RRL-PstI-For (5′CACCGGTATCGATA ATCTAGATTTGACGCGTCGAACTAGTCTGTCGGA GGAC TGGCGCGCCGAGTGAGG and 5′TAGCCTCG AGCTAGCTGCAGTAACGCCA), respectively. The final product C was obtained by using overlapping products A and B as templates and flanking primers RRL-PstI-For

and RRL-ApaI-Rev. Finally, product C was subcloned, sequenced, and cloned into pRRL-PPT-SF-IRES-EGFP-PRE by *Apa*I and *Pst*I restriction enzymes, resulting in pRRL-PPT-SF-newMCS-IRES-EGFP-PRE. For virus particle production, HEK293T cells were transfected with pRRL-PPT-SF-newMCS-i2-EGFPpre (empty vector backbone as control or vector containing subcloned human CalDAG GEFI) as well as packaging and envelope plasmids, employing calcium phosphate coprecipitation. Virus supernatant (VSN) was collected and concentrated via overnight centrifugation. For transduction, 2×10^6 Jurkat T cells were resuspended in 2 ml of enriched VSN and centrifuged for 30 min at 800 g. VSN was aspirated, and Jurkat T cells were cultured for 72 h in RPMI with 10% FCS before functional assays were performed. Transfection and transduction efficiencies were assessed via GFP expression of HEK293T and Jurkat T cells, respectively.

Adhesion and migration assays

JE6 or CalDAG GEFI$^{-/-}$ Jurkat T cells were adjusted to 1×10^5 cells/ml in RPMI with 10% FCS one day before the experiment. To study cell adhesion, on the experimental day, cells were stimulated with 5 µg/ml anti-CD3 (OKT3, BD Biosciences), 50 ng/ml PMA (Calbiochem), or 1 mM $MnCl_2$ for 30 min at 37 °C before adhesion on Fc-ICAM-1-coated (0.5 µg/well, R&D system) or Fibronectin-coated (1 µg/well, Roche) 96-well plates. 2×10^5 cells were seeded per well, and adhesion was allowed for 30 min at 37 °C. Unbound cells were removed by gently washing three times with HBSS (Biochrom AG), and the bound cell fraction was determined by counting using an ocular reticle. Bound cells were calculated as "% of input" in duplicates. Migration assays were performed using 5 µm polycarbonate filter transwells (Costar) coated with 20 µg/ml fibronectin (1 h 37 °C, Roche). The lower transwell chamber was filled with either migration assay medium (RPMI, 1% bovine serum albumin fraction V, 10 mM HEPES pH 7.4) or migration assay medium supplemented with 200 ng/ml human SDF-1α (CXCL12, Biolegend). 2×10^5 cells were added to the upper chamber in 200 µl migration assay medium, and after 2.5 h at 37 °C, the number of migrated cells into the lower chamber was counted.

Phosphotyrosine analysis

Total CD4$^+$ T cells were isolated from spleen and LNs of CalDAG GEFI$^{-/-}$, CalDAG GEFI$^{+/-}$ and CalDAG GEFI$^{+/+}$ mice using mouse CD4 DirectBeads (L3T4) and the autoMACS separation system (Miltenyi Biotec). For stimulation, 1×10^6 cells were resuspended in complete RPMI (cRPMI; 10% FCS, 25,000 Units penicillin/25 mg streptomycin, 1 mM sodium pyruvate, 25 mM HEPES, 50 µM β-mercaptoethanol) supplemented with either 20 ng/ml PMA and 1 µg/ml ionomycin (both from Sigma) or 35 µM sodium pervanadate (Sigma), and incubated for 5 min at 37 °C. For anti-CD3/CD28 stimulation, cells were coated with 20 µg/ml biotinylated anti-CD3 (clone 145-2C11, BD Biosciences) and 10 µg/ml biotinylated anti-CD28 (clone 37.51, BD Biosciences), and crosslinking was induced for 5 min by addition of 10 µg/ml streptavidin in cRPMI. As stimulation controls, cells were either left on ice or incubated at 37 °C for 5 min in cRPMI. Following stimulation, cells were washed once in ice-cold PBS, and cell pellets were further processed for lysis and Western Blotting.

Phosflow staining for phospho-ERK1/2

Cells from spleen and LNs of CalDAG GEFI$^{-/-}$, CalDAG GEFI$^{+/-}$ and CalDAG GEFI$^{+/+}$ mice were stained for dead cells using the LIVE/DEAD Fixable Dead Cell Stain (Invitrogen) and subsequently for surface markers CD4 and CD25. Next, cells were coated with 10 µg/ml biotinylated anti-CD3 (clone 145-2C11, BD Biosciences) and 5 µg/ml biotinylated anti-CD28 (clone 37.51, BD Biosciences) for 15 min on ice. After removal of excess antibody, cells were pre-warmed to 37 °C and stimulation was initiated by addition of 10 µg/ml streptavidin in cRPMI. After indicated time points, cells were fixed (BD Biosciences Phosflow Lyse/Fix) and permeabilized (BD Biosciences Phosflow Perm Buffer III) according to the manufacturer's protocol. Cells were stained intracellularly for ERK1/2 pT202/pY204 or isotype control (both BD Biosciences Phosflow) and Foxp3 at 4 °C overnight.

In vitro *suppression assay*

CD4$^+$CD25$^+$ Tregs were sorted from spleen and LNs of CalDAG GEFI$^{-/-}$, CalDAG GEFI$^{+/-}$ and CalDAG GEFI$^{+/+}$ mice as described above. Sorted cells were pre-activated for 72 h by stimulation on plate-bound anti-CD3/CD28. For antibody coating, wells were incubated overnight at 4 °C with 50 µg/ml goat fraction to hamster IgG (MP Biomedicals), washed with PBS, and subsequently incubated for 1 h at 4 °C with 1 µg/ml anti-CD3 (clone 145-2C11, Biolegend) and 3 µg/ml anti-CD28 (clone 37.51, Biolegend). Sorted cells were cultured in cRPMI supplemented with 40 ng/ml IL-2 (R&D). Freshly sorted and Cell Trace™ Violet (CTV, Invitrogen)-labeled Tnaive (CD4$^+$CD25$^-$ CD62L^{high}) from CalDAG GEFI$^{+/-}$ mice were cocultured with pre-activated Tregs at indicated ratios in presence of T activator Beads (Life Technologies) in a ratio of one bead to two cells. On day four, CTV dilution was determined in living Tnaive by flow cytometry.

Transfer colitis

Freshly sorted Tregs and Tnaive from CalDAG GEFI$^{-/-}$ and CalDAG GEFI$^{+/+}$ were washed in PBS, and a total of 4×10^5 cells was injected intraperitoneally into Rag2$^{-/-}$ recipient mice in a ratio of 1:2 or 1:4 (Tregs:Tnaive). Body

weight and health status of recipient mice was monitored biweekly over 10 weeks, and mice that lost >20% of initial body weight were sacrificed. For analysis, colon was rolled into a "Swiss roll", fixed in 4% neutrally buffered formaldehyde, and embedded in paraffin. Approximately 3-µm-thick sections were stained with hematoxylin/eosin (H&E) according to standard laboratory procedures. Slides were evaluated in a manner that was randomized and blinded to the experimental groups. A semi-quantitative score was applied for the marker's severity, lymphocytic invasion, epithelial hyperplasia, single cell apoptosis, and area involved. Each marker was graded from 0 to 3 as follows: Severity: 0 = no alteration, 1 = mild alteration, no serious disruption of the normal architecture, 2 = moderate alteration, but normal architecture of the epithelium still visible, 3 = severe inflammation disturbing the entire epithelial structure, transmural. Lymphocytic infiltration: 0 = no lymphocytes in lamina propria, 1 = few cells in lamina propria, not interfering with crypt structure, 2 = moderate amount of cells in lamina propria, increasing thickness of the crypts in max. 50%, 3 = transmural invasion of inflammatory cells, exceeds 2. Hyperplasia: 0 = no alteration, 1 = up to 50% increase in crypt length, 2 = 50–100% increase in crypt length, moderate disturbance of crypt architecture, 3 = more than 100% increase in crypt length and marked disturbance of crypt architecture. Single cell apoptosis: 0 = no apoptosis observed, 1 = max. 1 per crypt, 2 = 2–3 per crypt, 3 = exceeds 2. Area involved: 0 = no alteration, 1 ≤ 40%, 2 = 40–70%, 3 ≥ 70%. The grades for these markers were added together for a total score of 0–15.

Statistical analysis

Prism software (GraphPad) was employed for generation of graphs and statistical analysis. Data points in scatter plots represent individual mice. If not stated otherwise, data are represented as mean ± SD. Statistical significance was determined via Mann–Whitney test or one-way ANOVA (Bonferroni's multiple comparison test or Kruskal–Wallis with Dunn's test for multiple comparison). *p < 0.05 was considered significant with *p < 0.05, **p < 0.01, and ***p < 0.001.

Ethics

Animals were handled with appropriate care and welfare in accordance with good animal practice as defined by FELASA and the national animal welfare body GVSO-LAS under supervision of the institutional animal welfare officer, and all efforts were made to minimize suffering. Animal experiments were performed in accordance with institutional, state, and federal guidelines, and all animal experiments were approved by the Lower Saxony Committee on the Ethics of Animal Experiments as well as the responsible state office (Lower Saxony State Office of Consumer Protection and Food Safety) under the permit number 33.92-42502-04-13/1170.

Results

CalDAG GEFI is phosphorylated at Y523 and becomes dephosphorylated in Tregs upon TCR stimulation

CalDAG GEFI is known to have an impact on LFA-1 activation, showing responsiveness to both TCR and chemokine receptor triggering in human T cells [11, 14, 15]. However, the role of CalDAG GEFI in murine T cells and particularly in Tregs has not been studied so far, as no experimental evidence was available, showing that CalDAG GEFI is expressed in T cells from mice [5, 12]. Interestingly, we could detect CalDAG GEFI expression in *ex vivo*-isolated murine Tregs and Tconv during a recently performed comparative proteome study (manuscript under preparation), with a slightly higher expression level in Tconv *(Fig. 1a)*, a finding that could be confirmed by Western Blot analysis *(Fig. 1b)*. Quantitative phosphopeptide sequencing of unstimulated versus stimulated Tregs and Tconv within the same study (van Ham et al., under preparation) even led to the identification of a novel phosphorylation site within the C-terminal C1 domain of CalDAG GEFI at Y523 *(Fig. 1c)*. In resting Tregs, Y523 phosphorylation is slightly reduced as compared to resting Tconv. This difference becomes more pronounced upon TCR stimulation via crosslinked anti-CD3/CD28. Normalization to unstimulated Tconv shows that, while in Tconv Y523 phosphorylation is not responsive to TCR stimulation, the site gets strongly dephosphorylated in Tregs upon TCR triggering *(Fig. 1c,d)*. Thus, we confirm here that CalDAG GEFI is expressed at detectable levels in murine T cell subsets and we could identify a novel phosphorylation site located in the C1 domain that is differentially regulated downstream of TCR signaling in primary murine Tregs and Tconv.

Phosphorylation status of Y523 does not affect DAG binding of CalDAG GEFI C1 domain

Although it is well established that generally C1 domains bind DAG, it is not clear whether the C1 domain of CalDAG GEFI is responsive to this lipid second messenger or any of its derivatives, such as PMA [14, 30–33]. Recently, Czikora et al. showed that the C1 domain of human CalDAG GEFI binds DAG with very low affinity, if it indeed binds at all, which they primarily attribute to four amino acid residues, namely N505, S506, A517, and I519 [16]. As Y523 is in close proximity to these crucial amino acid residues that comprise part of the DAG-binding pocket, we wondered whether the phosphorylation status, which affects the local charge of the evolutionary conserved C1 domain *(Fig. 1e)*, influences the DAG-binding ability of CalDAG GEFI.

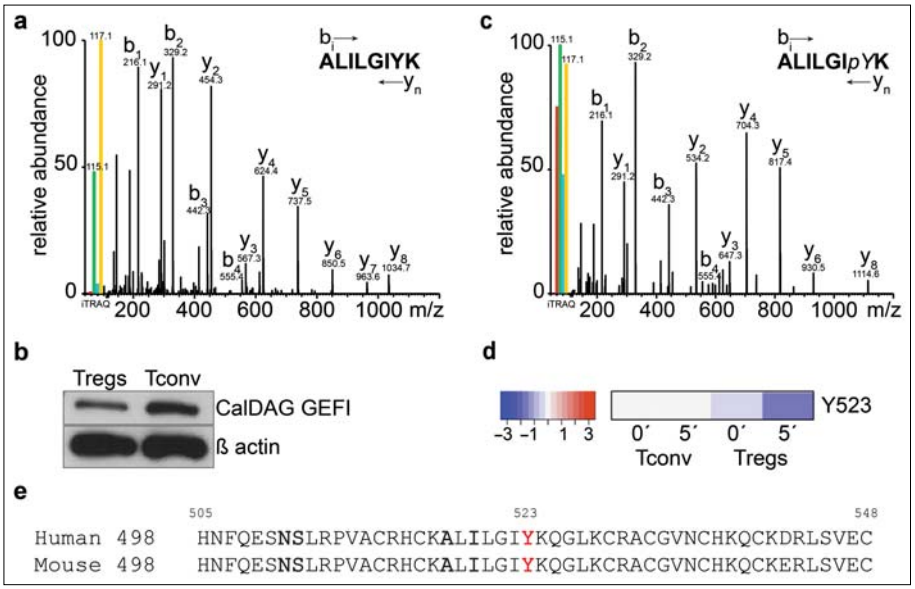

Fig. 1. CalDAG GEFI is expressed in primary murine Tregs and Tconv and is differentially phosphorylated upon TCR ligation. A comparative proteomic analysis of FACS-sorted primary murine Tregs and Tconv was performed and found CalDAG GEFI expression in both T cell subsets. (a) Representative MS/MS spectra of one of the identified iTRAQ-labeled peptides of murine CalDAG GEFI (Tregs 115.1 green, Tconv 117.1 yellow) and (b) Western blot for CalDAG GEFI from FACS-sorted primary murine Tregs and Tconv. β-Actin served as loading control. Quantitative phosphopeptide sequencing of unstimulated or anti-CD3/28 stimulated primary murine Tregs and Tconv identified a novel phosphorylation site within CalDAG GEFI at Y523. (c) Representative MS/MS spectra of the iTRAQ-labeled peptide of CalDAG GEFI, which covers the newly identified phosphorylation site at Y523 (iTRAQ ions: 114.1 resting Tregs, red; 115.1 resting Tconv, green; 116.1 activated Tregs, blue; 117.1 activated Tconv, yellow). The phosphorylation is apparent from the 80 Da difference in molecular weight of the peptide y2 (534.2 Da) as compared to peptide y2 in *Fig. 1a* (454.3 Da). The phosphorylation site Y523 is differentially regulated in primary Tregs and Tconv, especially following TCR triggering. (d) Direct comparison of the phosphorylation level of Y523 in resting (0´) and 5 min activated Tregs and Tconv (5´) revealed a reduced phosphorylation level of this site in Tregs when compared to Tconv, which becomes more pronounced after TCR ligation. (e) Comparison of the C1 domain protein sequence of CalDAG GEFI shows a high degree of conservation between humans and mice. Amino acids which were previously described to be important for DAG binding of C1 domains of CalDAG GEF family members are depicted as bold letters, and the newly identified phosphorylated residue Y523 is highlighted in red

To address this question, we cloned WT and two phosphomutant murine C1 domain constructs (Y523D and Y523F) into pGEX-4T-1, which adds an N-terminal GST-tag. Recombinant proteins were expressed in *E. coli* BL21, purified via sepharose, and eluted to high purity. We applied equal amounts of purified proteins to membrane lipid PIP Strips and detected protein binding to the spotted lipids via the GST-tag. For both mutated C1 domain versions, Y523D and Y523F, no DAG binding could be detected *(Fig. 2a)*. To support proper protein folding and stability, purified C1 domains were dialyzed against ZnCl2-containing buffer; however, this treatment did not result in any DAG bind-

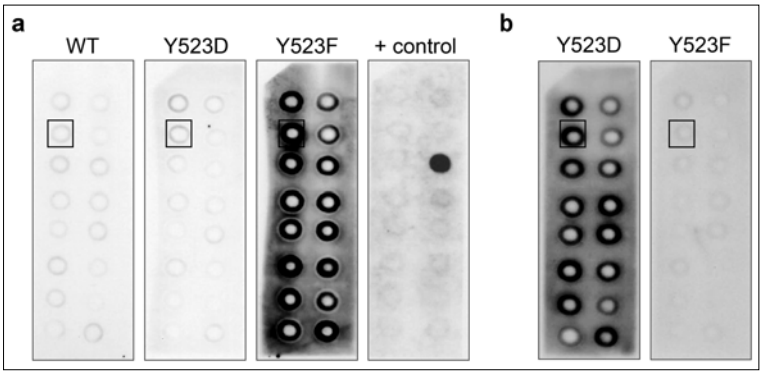

Fig. 2. Substitutions of CalDAG GEFI Y523 do not affect DAG binding of the C1 domain. The influence of the phosphorylation status of Y523 within the CalDAG GEFI C1 domain on binding to DAG was assessed. Membrane lipid PIP strips of recombinantly expressed and purified WT C1, phosphomimetic Y523D C1 and Y523F C1 domain, which represents the dephosphorylated state, as well as the manufacturer's positive control (+ control), are depicted. The tested proteins did not show binding to DAG (squares), neither (a) in absence nor (b) in presence of $ZnCl_2$, which aids in proper protein folding. Variation in background staining is in accordance with the methodology; a positive signal is attributed to an intense signal covering the full lipid spot (see + control). Data are representative of two independent experiments

ing of the phosphomutant versions of CalDAG GEFI C1 domain *(Fig. 2b)*. Therefore, we conclude that the observed differential phosphorylation of CalDAG GEFI Y523 in activated murine Tregs versus Tconv has no impact on CalDAG GEFI's sensitivity towards DAG.

CalDAG GEF$^{-/-}$ Jurkat T cells display slightly reduced TCR-induced adhesion to ICAM-1 and fibronectin but unaffected CXCR4-mediated migration

We generated two CalDAG GEFI$^{-/-}$ Jurkat T cell lines utilizing the CRISPR-Cas9 technology with transient expression of EGFP reporter protein, sgRNA and SpCas9 protein. Single GFP^{+} Jurkat T cells were FACS-sorted into 96-well plates and subsequently expanded. Loss of CalDAG GEFI expression in two established lines, namely, 2D5 (hereafter referred to as no. 1) and 3D6 (no. 2), was verified via Western blot analysis *(Suppl. Fig. 1a)*. CalDAG GEFI is implemented into signaling pathways leading to LFA-1 activation, and it was previously shown that siRNA-based silencing of CalDAG GEFI expression in Jurkat T cells impairs cell adhesion [15]. Therefore, we tested adhesion of CalDAG GEFI-deficient Jurkat T cell clones to ICAM-1 and fibronectin in comparison to WT Jurkat T cells (JE6). As expected, unstimulated Jurkat

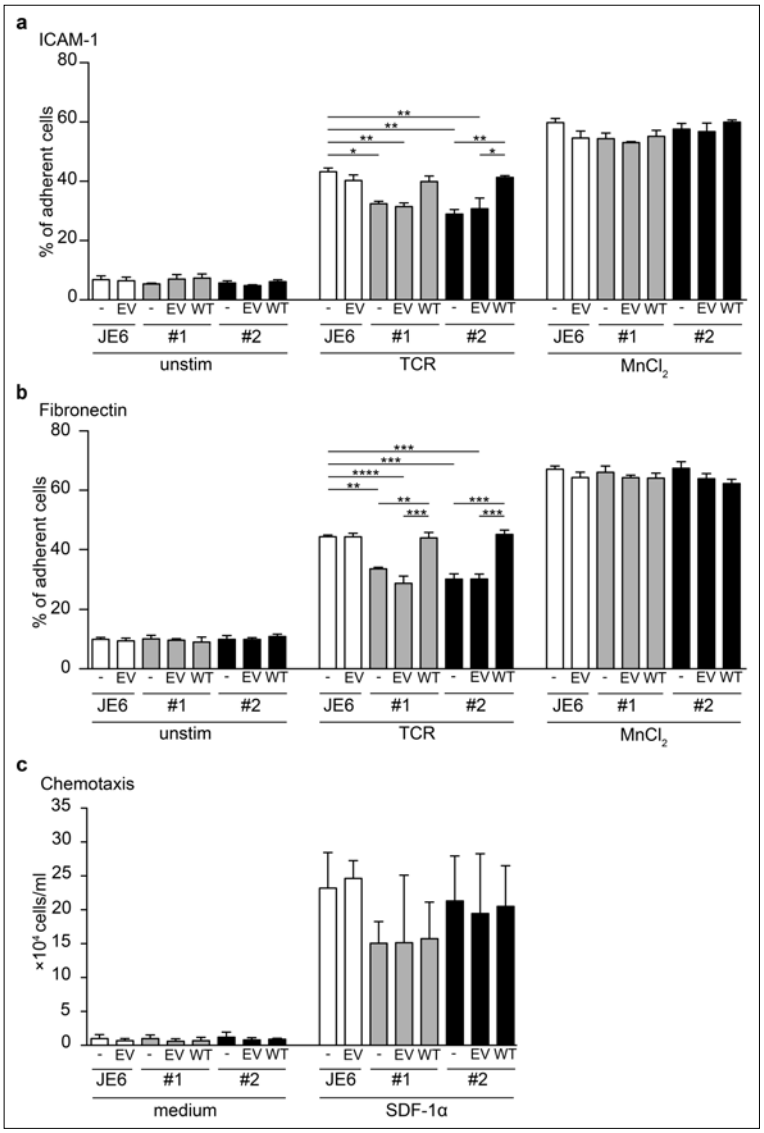

Fig. 3. CalDAG GEFI$^{-/-}$ Jurkat T cells show slightly reduced adhesion but unaffected migration properties. Two CalDAG GEFI$^{-/-}$ Jurkat T cell clones were generated and tested for adhesion to ICAM-1 and fibronectin as well as for migration on fibronectin towards a chemoattractant. To rescue adhesion and/or migration abnormalities caused by CalDAG GEFI knock-out, both CalDAG GEFI$^{-/-}$ clones were reconstituted with wildtype CalDAG GEFI. Transduction with empty vector backbone served as treatment control. CalDAG GEFI-competent JE6 Jurkat T cells (JE6, white bars) or CalDAG GEFI$^{-/-}$ clones (no. 1, grey bars, and no. 2, black bars), untransduced (−), empty vector transduced (EV) or CalDAG GEFI reexpressing (WT), were either left unstimulated (unstim) or were stimulated via anti-CD3 (TCR) or $MnCl_2$ ($MnCl_2$) to induce adhesion to (a) ICAM-1 or (b) fibronectin. (c) JE6 and CalDAG GEFI$^{-/-}$ clones, untransduced and transduced, were tested for migration without chemoattractant (medium) or towards SDF-1α. Data are pooled from three to five independently performed experiments (mean ± SD)

T cells showed very little adhesion, while nearly 60% of $MnCl_2$-treated cells attached to ICAM-1 and fibronectin irrespective of CalDAG GEFI deficiency. Deficiency of CalDAG GEFI led to significantly reduced adhesion of TCR-triggered Jurkat T cells to both ICAM-1 and fibronectin *(Fig. 3a,b)*. Importantly, this phenotype could be reverted and rescued upon lentiviral reexpression of CalDAG GEFI (WT), while transduction with an empty control vector (EV) did not show any effect *(Fig. 3a,b)*. As it was already reported that LFA-1 activation is also required for CXCR4-mediated chemotaxis towards SDF-1α [34], we next analyzed the impact of CalDAG

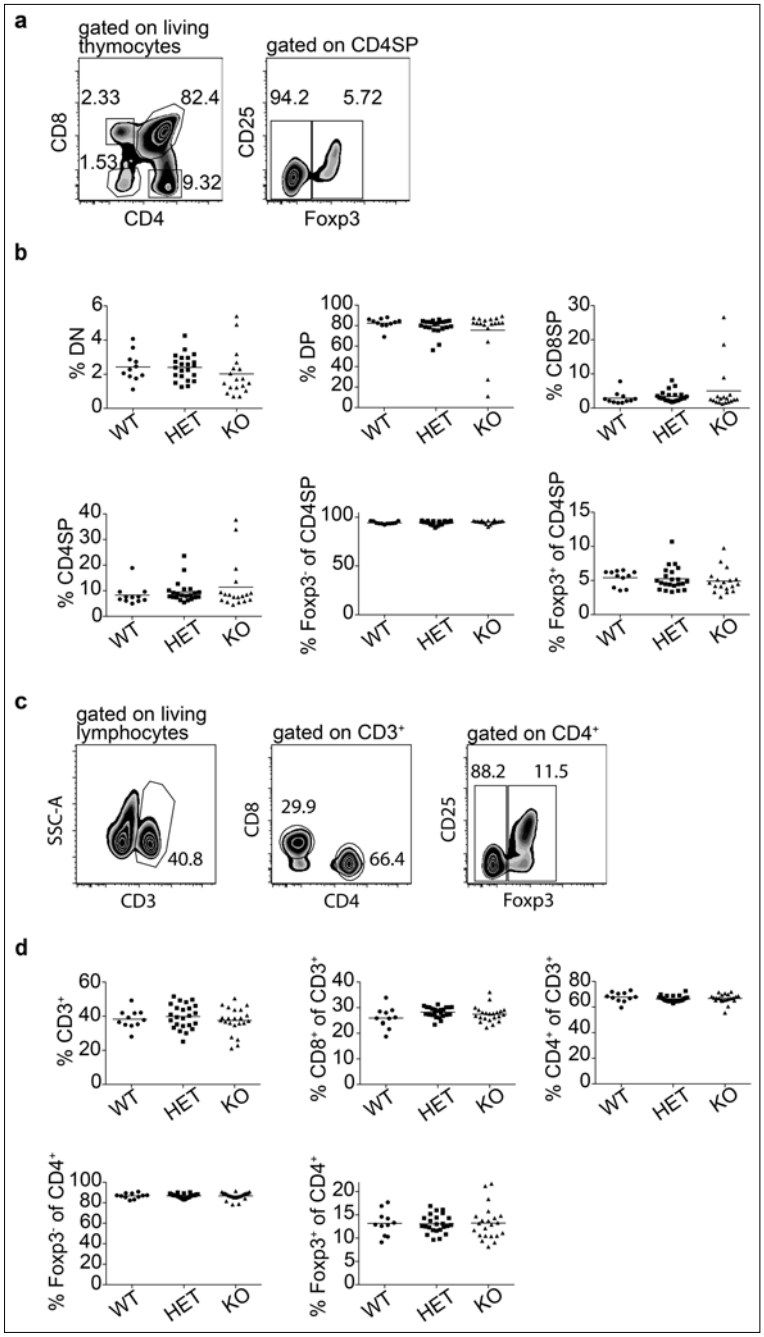

Fig. 4. Thymic T cell development and peripheral T cell homeostasis are unaffected by CalDAG GEFI deficiency. Flow cytometry data of the T cell compartment of single cell suspensions from (a, b) thymus and (c, d) pooled spleen and LNs from CalDAG GEFI$^{+/+}$ (WT), CalDAG GEFI$^{+/-}$ (HET), and CalDAG GEFI$^{-/-}$ (KO) mice. (a) Exemplary dot plots show CD4 versus CD8 expression on gated living thymocytes (left) and Foxp3 versus CD25 expression on gated CD4SP thymocytes (right). (b) Scatter plots summarize frequencies of DN, DP, CD8SP, total CD4SP, Foxp3$^-$CD4SP, and Foxp3$^+$CD4SP thymocytes from CalDAG GEFI$^{+/+}$ (WT), CalDAG GEFI$^{+/-}$ (HET), and CalDAG GEFI$^{-/-}$ (KO) mice (n = 11–21 per group). (c) Exemplary dot plots show CD3 expression on gated living pooled spleen and LN cells (left), CD4 versus CD8 expression on gated CD3$^+$ cells (middle) and CD25 versus Foxp3 expression on gated CD3$^+$CD4$^+$ cells (right). (d) Scatter plots summarize frequencies of CD3$^+$, CD8$^+$, total CD4$^+$, Foxp3$^-$CD4$^+$, and Foxp3$^+$CD4$^+$ cells from pooled spleen and LN cells from CalDAG GEFI$^{+/+}$ (WT), CalDAG GEFI$^{+/-}$ (HET), and CalDAG GEFI$^{-/-}$ (KO) mice (n = 11–24 per group). Mean of each group is depicted, and each data point represents a single mouse

GEFI expression on the migration capability of Jurkat T cells. In absence of a chemoattractant, all analyzed cells showed comparable basal migration *(Fig. 3c)*. However, in the presence of SDF-1α, both CalDAG GEFI$^{-/-}$ clones showed slightly diminished migration towards the chemokine, which could not be rescued by reexpression of CalDAG GEFI *(Fig. 3c),* suggesting that this phenotype is clone-specific and not due to CalDAG GEFI deficiency. To rule out the possibility that reduced adhesion and migration of CalDAG GEFI$^{-/-}$ clones are due to a reduction in surface expression of molecules that are involved in the respective signaling pathways, we analyzed protein abundance of CD3, the LFA-1 component CD11a, and the SDF-1α receptor CXCR4 on JE6 Jurkat T cells and both CalDAG GEFI$^{-/-}$ clones via flow cytometry. No significant differences in surface expression of CD3 and CXCR4 could be detected, and reexpression of CalDAG GEFI by lentiviral transduction had no influence on these molecules *(Suppl. Fig. 1b,c,e)*. However, differences could be observed with regard to CD11a, whose expression was significantly reduced on clone no. 1 independent of the lentiviral reexpression *(Suppl. Fig. 1d)*. Taken together, we conclude that the drop in surface levels of CD11a is biologically irrelevant in the experimental settings used

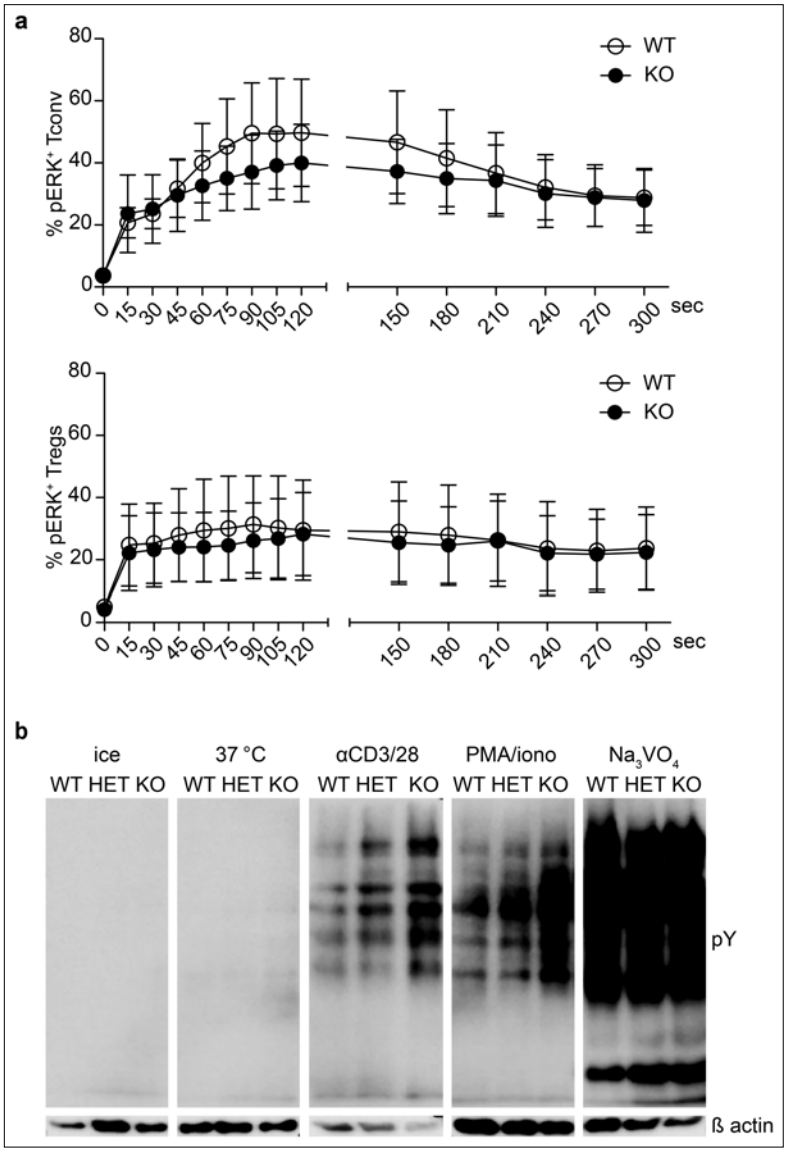

Fig. 5. Signal transduction is comparable in CD4$^+$ T cells from CalDAG GEFI$^{+/+}$ and CalDAG GEFI$^{-/-}$ mice. Phosphorylation of ERK was assessed by flow cytometry of bulk CD4$^+$ T cells, which were stimulated via crosslinking of biotinylated anti-CD3/CD28 via streptavidin over a time course of 5 min. Tconv and Tregs were gated separately according to Foxp3 expression. (a) Graphs summarize frequencies of pERK$^+$ cells at indicated time points for Tconv (upper panel) and Tregs (lower panel) (mean ± SD; n = 10 mice per group); CalDAG GEFI$^{+/+}$ (WT, open circles) and CalDAG GEFI$^{-/-}$ (KO, closed circles). (b) Total CD4$^+$ cells from spleen and LNs from CalDAG GEFI$^{+/+}$ (WT), CalDAG GEFI$^{+/-}$ (HET), and CalDAG GEFI$^{-/-}$ (KO) mice were stimulated for 5 min, and total phosphorylated tyrosine residues (pY) were analyzed via Western blot. As stimulation controls, cells were either kept on ice or incubated for 5 min at 37 °C. Activation of cells was carried out via crosslinking of biotinylated anti-CD3/CD28 via streptavidin (αCD3/28), PMA, or pervanadate (Na_3VO_4). β-Actin served as loading control. Exemplary Western blots from three independent experiments are shown

in the present study to analyze cell adhesion and chemotaxis, suggesting that loss of CalDAG GEFI impairs LFA-1-dependent adhesion of Jurkat T cells to ICAM-1 and fibronectin following TCR triggering, whereas CXCR4-mediated migration remains unaffected.

CalDAG GEFI$^{-/-}$ mice display normal thymic T cell development and T cell homeostasis in secondary lymphoid organs

To address the role of CalDAG GEFI in murine T cells apart from the differential phosphorylation dynamics at Y523 in Tregs, we analyzed the T cell compartment within CalDAG GEFI$^{-/-}$ mice, which had been previously reported to have defects in platelet aggregation and neutrophil migration [12, 13]. In these initial studies, the lymphocyte count appeared to be normal, although the T cell compartment was not analyzed in detail [12]. Here, we first analyzed the thymic T cell compartment and did not observe any overt effect of CalDAG GEFI deficiency on T cell development, as double negative (DN), double positive (DP), CD8 single positive (CD8SP), and CD4 single positive (CD4SP) fractions were found in comparable frequencies in CalDAG GEFI$^{-/-}$ (KO), CalDAG GEFI$^{+/-}$ (HET), and CalDAG GEFI$^{+/+}$ (WT) mice *(Fig. 4a,b)*. Similarly, no differences in frequencies of Foxp3^{+} and Foxp3^{-} CD4SP thymocyte subsets were found *(Fig. 4a,b),* and also the two Treg precursors identified as CD25^{+}Foxp3^{-} or CD25^{-} Foxp3^{+} cells [35, 36] were present at comparable frequencies (data not shown). To assess the impact of CalDAG GEFI deficiency on T cell homeostasis in the periphery, we analyzed the T cell compartment in pooled spleen and LNs and observed no differences in frequencies and absolute numbers of CD3^{+}, CD4^{+}, CD8^{+}, CD4^{+}Foxp3^{-}, and CD4^{+}Foxp3^{+} T cell subsets in WT, HET, and KO mice *(Fig. 4c,d,* and data not shown*)*. We conclude that deficiency of CalDAG GEFI affects neither thymic development nor peripheral homeostasis of T cells.

TCR downstream signaling is not affected by loss of CalDAG GEFI

It was previously reported that CalDAG GEFI affects ERK1/2 activation via Rap1, and, more specifically, it

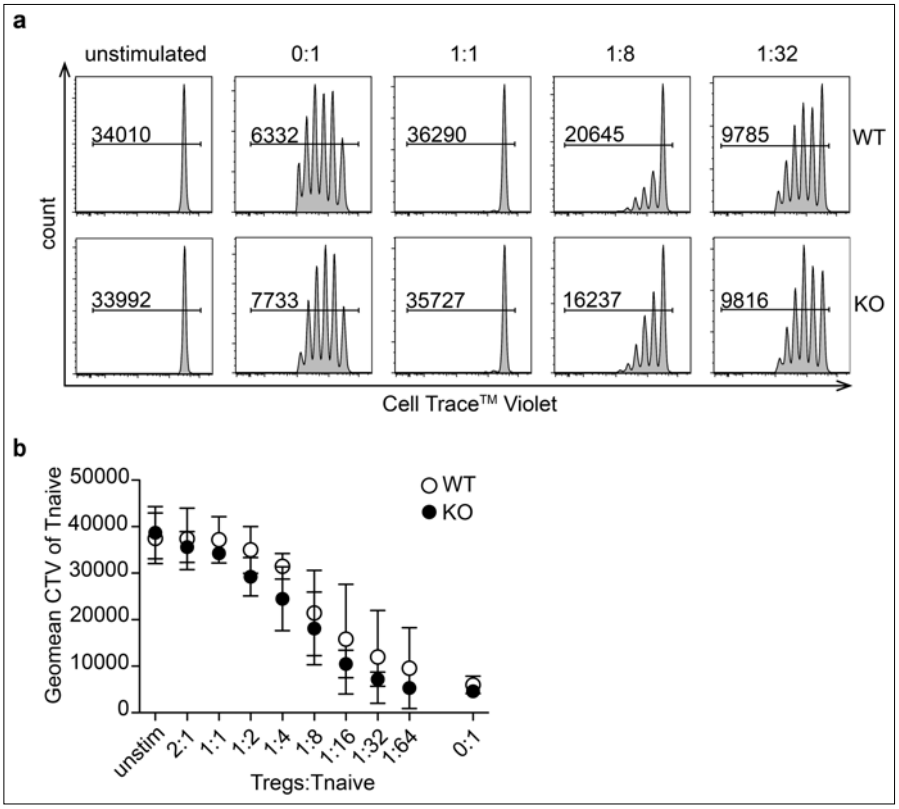

Fig. 6. CalDAG GEFI$^{-/-}$ Tregs are suppressive *in vitro*. Ability of Tregs from CalDAG GEFI$^{+/+}$ and CalDAG GEFI$^{-/-}$ mice to suppress proliferation of bead-stimulated Tnaive from CalDAG GEFI$^{+/-}$ *in vitro* was compared. (a) Exemplary histogram plots show dilution of the proliferation dye cell trace violet (CTV) of bead-stimulated sorted Tnaive cells. Tnaive cells were cultured without addition of Tregs and without T activator beads (unstimulated) as negative proliferation control (far left). Coculture of Tnaive and Tregs at indicated ratios (Tregs: Tnaive at 0:1, 1:1, 1:8 and 1:32), including a constant number of T activator beads, displays comparable suppressive capability of CalDAG GEFI$^{+/+}$ (WT, upper panel) and CalDAG GEFI$^{-/-}$ (KO, lower panel) Tregs. Numbers indicate geometric mean (Geomean) of the respective signal intensity of CTV gated on total Tnaive cells. (b) Mean and standard deviation of the Geomean of CTV of Tnaive cocultured with CalDAG GEFI$^{+/+}$ (WT, open circles) and CalDAG GEFI$^{-/-}$ (KO, closed circles) Tregs. Data are pooled from three independently performed experiments (mean ± SD)

was shown that CalDAG GEFI reduces Elk1 activation and thereby limits ERK1/2 phosphorylation [9–11, 37]. As it is also known that Tregs display attenuated pERK1/2 levels as compared to Tconv [26, 27, 38], we sought to address the role of CalDAG GEFI in TCR downstream signaling in *ex vivo* isolated Tregs and Tconv. To this end, we stimulated total $CD4^+$ T cells from pooled spleen and LNs of CalDAG $GEFI^{-/-}$ (KO) or CalDAG $GEFI^{+/+}$ (WT) mice via crosslinking of anti-CD3/CD28. At various time points following stimulation, we measured pERK1/2 via flow cytometry in $Foxp3^+$ and $Foxp3^-$ $CD4^+$ T cell subsets. As expected, ERK1/2 phosphorylation was induced rapidly upon TCR ligation in both Tregs and Tconv, with Tconv reaching higher frequencies of $pERK^+$ cells when compared to Tregs *(Fig. 5a,b)*. Interestingly, CalDAG GEFI deficiency did not affect ERK1/2 phosphorylation significantly, neither in Tconv nor in Tregs, although a trend towards reduced ERK1/2 phosphorylation was observed in Tconv from CalDAG GEFI-deficient mice (KO) *(Fig. 5a)*. To get a more global picture on the impact of CalDAG GEFI on TCR downstream signaling events, we next analyzed total tyrosine phosphorylation patterns by Western blotting in stimulated total $CD4^+$ T cells *ex vivo* isolated from pooled spleen and LNs of CalDAG $GEFI^{-/-}$ (KO), CalDAG $GEFI^{+/-}$ (HET), and CalDAG $GEFI^{+/+}$ (WT) mice. Isolated cells were stimulated via crosslinking anti-CD3/CD28 for 5 min, and stimulations using PMA/ionomycin or sodium pervanadate were taken as positive controls. Unstimulated cells, which were either kept on ice or incubated in medium only, did not show any signs of tyrosine phosphorylation *(Fig. 5b)*. For none of the tested stimulation conditions (anti-CD3/CD28, PMA/ionomycin, or sodium pervanadate), major differences in tyrosine phosphorylation could be observed when KO, HET, and WT $CD4^+$ T cells were compared, while expected alterations in overall signal strength according to the respective stimulation condition were apparent *(Fig. 5b)*. Thus, in our experimental setting, CalDAG GEFI is largely dispensable for TCR downstream signaling within primary murine $CD4^+$ T cells.

CalDAG $GEFI^{-/-}$ Tregs display normal suppressive capacity in vitro

To assess the suppressive capacity of CalDAG $GEFI^{-/-}$ Tregs *in vitro*, $CD4^+CD25^+$ Tregs were sorted from pooled spleen and LNs of CalDAG $GEFI^{-/-}$ or CalDAG $GEFI^{+/+}$ mice and pre-activated in presence of IL-2 for 72 h on plate-bound anti-CD3/CD28. Subsequently, pre-activated Tregs were cocultured with cell trace violet-labeled Tnaive (CTV) freshly isolated from CalDAG $GEFI^{+/-}$ mice in titrated ratios in presence of anti-CD3/CD28-coated beads. At day 4 of the coculture, proliferation of Tnaive was measured by analyzing CTV dilution via flow cytometry. As expected, unstimulated Tnaive did not proliferate and showed a high CTV fluorescence signal, while stimulated Tnaive in the absence of Tregs (0:1) proliferated substantially and diluted the dye progressively with every generation *(Fig. 6a,b)*. Upon addition of Tregs, a dose-dependent suppressive activity could be observed; however, no difference was apparent when Tregs from CalDAG $GEFI^{-/-}$ (KO) and CalDAG $GEFI^{+/+}$ (WT) mice were directly compared *(Fig. 6b)*. Foxp3 staining on the day of analysis revealed equal survival and stability of CalDAG $GEFI^{-/-}$ and CalDAG $GEFI^{+/+}$ Tregs in the respective cultures (data not shown). In conclusion, CalDAG GEFI deficiency does not alter the suppressive ability of the Tregs in this APC-free *in vitro* system. However, since CalDAG GEFI plays a crucial role in LFA-1 activation and this integrin has an important function in the formation of the IS between T cells and APCs, the effect of CalDAG GEFI deficiency on the suppressive capacity of Tregs might rely on their interaction with APCs.

CalDAG $GEFI^{-/-}$ Tregs are less capable to prevent intestinal inflammation in the transfer colitis model

To evaluate the suppressive capacity of CalDAG $GEFI^{-/-}$ Tregs under more physiological conditions, we chose the transfer colitis model, which is widely used to assess the suppressive capacity of Tregs. As expected, $Rag2^{-/-}$ recipient mice receiving only Tnaive from CalDAG $GEFI^{+/+}$ mice developed signs of colitis as evidenced by body weight loss starting from week 5 to 6 after T cell transfer *(Suppl. Fig. 2a)*, shortening of colon length *(Suppl. Fig. 2b)*, and a strong colonic pathology when compared to control mice receiving PBS only *(Fig. 7)*. Cotransfer of Tnaive with $CD4^+CD25^+$ Tregs at a ratio of 1 : 2 (Treg : Tnaive) resulted in a mild, but substantial amelioration of intestinal inflammation regarding all parameters tested; however, no differences could be observed between Tregs isolated from CalDAG $GEFI^{-/-}$ (KO) or CalDAG $GEFI^{+/+}$ (WT) mice *(Fig. 7a, Suppl. Fig. 2a,b)*. Accordingly, flow cytometric analysis of the T cell compartment in spleen, mLNs, and pLNs at the termination of the experiment did not show any differences in frequencies and absolute numbers of $CD3^+CD4^+$, $CD4^+CD44^+CD62L^-$ memory T cells, $CD4^+Foxp3^+$ Tregs, and $CD4^+Foxp3^-$ Tconv, as well as CD103 and CTLA-4 expression on Tregs (data not shown).

Next, we tested a lower ratio between Tregs and Tnaive (1:4), which has been used previously to detect subtle differences in the suppressive capacity of Treg subsets [39, 40]. Again, no differences with regard to body weight loss and colon length could be observed between the groups of mice receiving WT or KO Tregs *(Suppl. Fig. 2c,d)*. However, analysis of colonic pathology revealed that Tregs from CalDAG $GEFI^{-/-}$ mice had a slightly reduced suppressive capacity when compared to Tregs from CalDAG $GEFI^{+/+}$ mice *(Fig. 7b)*. Together, we conclude that CalDAG GEFI deficiency mildly affects the suppressive capacity of Tregs *in vivo,* with this phenotype only becoming apparent under weak suppression conditions.

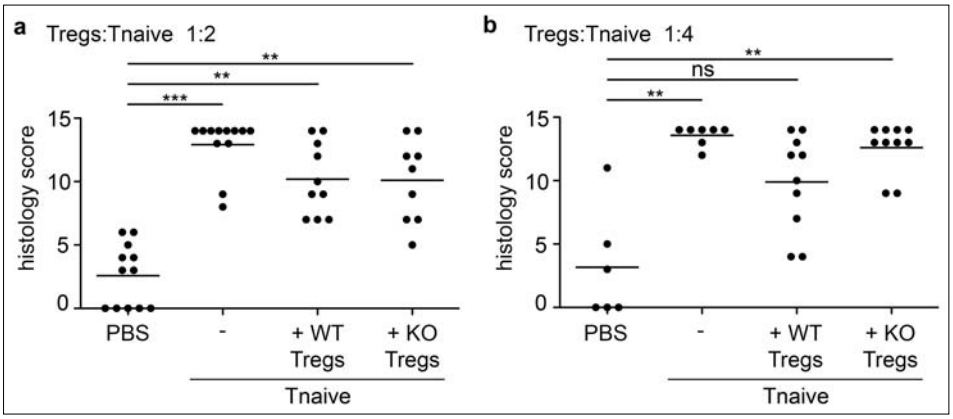

Fig. 7. Suppressive capacity of CalDAG GEFI$^{-/-}$ Tregs is slightly reduced in an *in vivo* model of transfer colitis. Capability of Tregs from CalDAG GEFI$^{+/+}$ and CalDAG GEFI$^{-/-}$ mice to suppress colon inflammation *in vivo* after cotransfer with Tnaive from CalDAG GEFI$^{+/+}$ into lymphopenic Rag2$^{-/-}$ mice was tested. PBS was injected as negative control (PBS). Eight to 10 weeks after T cell transfer, sections from colons were H&E stained and scored for severity of inflammation with a maximum score of 15. Rag2$^{-/-}$ mice received Tnaive from CalDAG GEFI$^{+/+}$ mice alone (no Tregs) or plus Tregs from either CalDAG GEFI$^{+/+}$ (WT Tregs) or CalDAG GEFI$^{-/-}$ (KO Tregs) mice at a ratio of (a) 1:2 or (b) 1:4 (Tregs:Tnaive). Means of histology scores within the indicated experimental groups are shown with each data point representing an individual mouse (pooled data from two independent experiments; n = 6–10 mice per group).

Discussion

CalDAG GEFI is known to be important for human T cell adhesion [15]. Yet, it has not been investigated whether it also has a specific role in Foxp3$^+$ Tregs. In the present study, we report on a novel phosphorylation site at Y523 within the C1 domain of mouse CalDAG GEFI, which upon stimulation is differentially regulated in *ex vivo* isolated murine Tregs when compared to Tconv. T cell development and homeostasis in secondary lymphoid organs, as well as ERK phosphorylation, are all unaffected in CalDAG GEFI$^{-/-}$ mice, and general signal transduction as seen by tyrosine phosphorylation patterns in total CD4$^+$ T cells is also unchanged. Although CalDAG GEFI$^{-/-}$ Jurkat T cells showed normal chemotaxis behavior when compared to CalDAG GEFI-expressing Jurkat T cells, their adhesion to ICAM-1 and fibronectin was impaired. These data correspond nicely to the assessment of the suppressive capacity of CalDAG GEFI$^{-/-}$ Tregs, which showed a normal inhibition of Tnaive proliferation in an APC-free *in vitro* assay, while a reduced suppressive capacity was observed at weak suppression conditions *in vivo*.

The CalDAG GEF family comprises four members, CalDAG GEFI-IV [12, 41–44]. Although CalDAG GEFI is not the most prominent family member to be found in T cells, in a recently performed study, we identified a novel phosphorylation site in CalDAG GEFI, which is located within its C-terminal C1 domain at Y523. Quantitative phosphopeptide sequencing comparing unstimulated and TCR-stimulated primary murine Tregs and Tconv revealed that Y523 phosphorylation is not affected by TCR stimulation in Tconv, whereas this site becomes strongly dephosphorylated upon TCR ligation in Tregs. As there is a growing body of evidence that TCR downstream signaling is distinctively organized in Tregs and Tconv [24, 26, 27, 38], we speculated whether this differential phosphorylation fosters a differential activation of the two T cell subsets while also promoting the formation of a Treg-specific IS. The specific kinase responsible for phosphorylating CalDAG GEFI at Y523 and which phosphatase dephosphorylates it upon TCR ligation specifically in Tregs remain unidentified, and further studies are needed for their identification. In contrast to the other family members, CalDAG GEFI contains an atypical C1 domain, and it is currently debated whether this C1 domain can bind DAG itself, or simply DAG derivatives such as PMA [14, 16, 30–33, 45]. Czikora et al. reported that the C1 domain of human CalDAG GEFI binds DAG with very low affinity [16]. They could identify four critical amino acids within the C1 domain, which were essential for conformational stability of the binding pocket and its ability to retain a phorbol ester within this pouch. These exact amino acids are N505, S506, A517, and I519, which are replaced by N505T, S506Y, A517G, and I519L within the C1 domain of CalDAG GEFII and enable DAG responsiveness of this GEF [16]. The importance of the residue S506 was also previously addressed by Johnson et al.; however, they came to the conclusion that amino acid variations alone cannot account for the total loss of phorbol ester binding [45]. As the differentially phosphorylated Y523 localized into the loop B of the phorbol ester-binding pouch, we speculated that the negative charge of the phosphogroup also contributes to the inability to bind DAG, and that DAG responsiveness of CalDAG GEFI might be restored in Tregs upon removal of the phosphorylation after TCR triggering, leaving the hydrophobic tyrosine as a suitable environment for lipid binding. We generated a phosphomimetic mutant, Y523D, and a mutant representing the dephosphorylated state, Y523F, of the C1 domain, and tested for DAG binding via membrane lipid PIP strips. As all of the mutant C1 domains showed detectable binding, the functional role of the differentially regulated phosphorylation at Y523 in Tconv and Tregs might be related to activation of the pro-

tein or interaction with other molecules, and needs to be addressed in future experiments.

We detected impaired adhesion of CalDAG GEFI$^{-/-}$ Jurkat T cell clones to ICAM-1 and fibronectin following TCR stimulation, and this phenotype could be reverted by reexpression of CalDAG GEFI. The observed decline in adhesiveness following TCR triggering was not due to disturbed expression of CD3, which could have accounted for impaired stimulation resulting in decreased integrin activation. Furthermore, although we saw a significant reduction in surface expression of CD11a on one of the CalDAG GEFI$^{-/-}$ Jurkat T cell clones, this observation was not influenced by reexpression of CalDAG GEFI. Therefore, we conclude that this phenotype was clone-specific and did not affect adhesion properties. Our finding that CalDAG GEFI plays a role in cell adhesion following TCR ligation is in line with published data showing CalDAG GEFI-mediated cell adhesion to ICAM-1 after SDF-1α stimulation [15]. In contrast to adhesion, chemokine-triggered migration of CalDAG GEFI$^{-/-}$ Jurkat T cells on fibronectin was not affected. Although a slightly lower number of migrating cells was observed for CalDAG GEFI$^{-/-}$ clones in the present study, the difference did not reach statistical significance and was not influenced by reexpression of CalDAG GEFI. Thus, we speculate that CalDAG GEFI plays a role in adhesion and stable IS formation in murine T cells, but is dispensable for migration processes and hemisynapse formation [2].

In CalDAG GEFI$^{-/-}$ mice, platelets display a reduced activation of Rap1, as well as deficits in attachment and thrombus formation due to impaired $\alpha_{II}\beta_3$ and β_1 integrin activation [12, 13, 46]. Furthermore, neutrophils of this mouse line are defective in migration, which was also attributed to reduced Rap1, β_1 and β_2 integrin activation, as well as decreased integrin and L-selectin expression [13, 46]. Lymphocyte counts appeared to be normal [12], and CalDAG GEFI$^{-/-}$ mice are lacking any obvious T cell-related phenotype. In line with these previously published general observations, more thorough examination of the T cell compartment within the thymus and secondary lymphoid organs confirmed that T cell development and homeostasis are not disturbed in CalDAG GEFI$^{-/-}$ mice, suggesting that, in T cells, CalDAG GEFI deficiency can be compensated for by other GEFs, like C3G [9, 47], and might play non-redundant roles only in specific cell types and/or under certain perturbations.

Several *in vitro* studies proposed a role for CalDAG GEFI in ERK1/2 activation [10, 11, 48]. Kawasaki et al. found that overexpression of CalDAG GEFI in 293T cells inhibits Elk1 activation and assumed that this would lead to reduced phosphorylation of ERK1/2 further downstream [10]. In this case, knock-out of CalDAG GEFI should result in elevated pERK1/2 levels, although this hypothesis could not be confirmed utilizing primary murine CD4$^+$ T cells from CalDAG GEFI$^{-/-}$, CalDAG GEFI$^{+/-}$, and CalDAG GEFI$^{+/+}$ mice in the present study. Generally, we could not detect a direct link between loss of CalDAG GEFI expression in murine CD4$^+$ T cells and any impairment of signal transduction. A more recent publication described a negative feedback loop, in which ERK1/2 phosphorylates CalDAG GEFI at S394, which in turn auto-inhibits its GEF activity towards Rap1, ultimately also reducing phosphorylation of ERK1/2 [48]. However, in our phosphoproteomic approach, we could not identify any phosphorylation of S394, indicating that, under the applied stimulation conditions, ERK1/2 does not phosphorylate S394 in murine CD4$^+$ T cells.

CalDAG GEFI-deficient Tregs showed a comparable suppressive capacity as Tregs from WT mice when tested *in vitro*, suggesting that the mere absence of this molecule does not dramatically affect the functional properties of these cells in an APC-free system. However, when CalDAG GEFI-deficient Tregs were tested *in vivo* under conditions that allow detection of subtle differences in the suppressive capacity of Treg subsets [39, 40], a slightly reduced inhibition of intestinal inflammation was observed when compared to WT Tregs, indicating that CalDAG GEFI fine-tunes the functional properties of Tregs, most likely through the modulation of aggregate formation between Tregs and APCs, a process known to strongly affect the suppressive function of Tregs [49].

In conclusion, our data suggest that CalDAG GEFI is dispensable for LFA-1 activation during migratory processes in CD4$^+$ T cells, but is crucial for fine-tuning LFA-1 activation at the IS. Whether the differential phosphorylation at Y523 in Tconv and Tregs contributes to the formation a Tregs-specific IS needs to be addressed in future studies.

Funding sources

This work was supported by the German Research Foundation (Collaborative Research Centre 854; project B12 to S.K. and C.F., project B16 to L.J. and J.H.) and the Gradschool GS-FIRE of the Helmholtz Centre for Infection Research Braunschweig.

Conflict of interest

The authors declare no conflict of interest.

Acknowledgements

We thank Maria Ebel, Beate Pietzsch, and Anke Ramonat for excellent technical
assistance.

References

1. Brownlie RJ, Zamoyska R: T cell receptor signalling networks: branched, diversified and bounded. Nat Rev Immunol 13, 257–269 (2013)

2. Dustin ML: A dynamic view of the immunological synapse. Semin Immunol 17, 400–410 (2005)
3. Graf B, Bushnell T, Miller J: LFA-1-mediated T cell costimulation through increased localization of TCR/class II complexes to the central supramolecular activation cluster and exclusion of CD45 from the immunological synapse. J Immunol 179, 1616–1624 (2007)
4. Bachmann MF, McKall Faienza K, Schmits R, Bouchard D, Beach J, Speiser DE, Mak TW, Ohashi PS: Distinct roles for LFA-1 and CD28 during activation of naive T cells: Adhesion versus costimulation. Immunity 7, 549–557 (1997)
5. Hogg N, Patzak I, Willenbrock F: The insider's guide to leukocyte integrin signalling and function. Nat Rev Immunol 11, 416–426 (2011)
6. Alon R, Dustin ML: Force as a facilitator of integrin conformational changes during leukocyte arrest on blood vessels and antigen-presenting cells. Immunity 26, 17–27 (2007)
7. Feigelson SW, Pasvolsky R, Cemerski S, Shulman Z, Grabovsky V, Ilani T, Sagiv A, Lemaitre F, Laudanna C, Shaw AS, Alon R: Occupancy of lymphocyte LFA-1 by surface-immobilized ICAM-1 is critical for TCR- but not for chemokine-triggered LFA-1 conversion to an open headpiece high-affinity state. J Immunol 185, 7394–7404 (2010)
8. Tan SM: The leucocyte beta2 (CD18) integrins: the structure, functional regulation and signalling properties. Biosci Rep 32, 241–269 (2012)
9. Hattori M, Minato N: Rap1 GTPase: functions, regulation, and malignancy. J Biochem 134, 479–484 (2003)
10. Kawasaki H, Springett GM, Toki S, Canales JJ, Harlan P, Blumenstiel JP, Chen EJ, Bany IA, Mochizuki N, Ashbacher A, Matsuda M, Housman DE, Graybiel AM: A Rap guanine nucleotide exchange factor enriched highly in the basal ganglia. Proc Natl Acad Sci U S A 95, 13278–13283 (1998)
11. Katagiri K, Shimonaka M, Kinashi T: Rap1-mediated lymphocyte function-associated antigen-1 activation by the T cell antigen receptor is dependent on phospholipase C-gamma1. J Biol Chem 279, 11875–11881 (2004)
12. Crittenden JR, Bergmeier W, Zhang Y, Piffath CL, Liang Y, Wagner DD, Housman DE, Graybiel AM: CalDAG-GEFI integrates signaling for platelet aggregation and thrombus formation. Nat Med 10, 982–986 (2004)
13. Bergmeier W, Goerge T, Wang HW, Crittenden JR, Baldwin AC, Cifuni SM, Housman DE, Graybiel AM, Wagner DD: Mice lacking the signaling molecule CalDAG-GEFI represent a model for leukocyte adhesion deficiency type III. J Clin Invest 117, 1699–1707 (2007)
14. Caloca MJ, Zugaza JL, Vicente-Manzanares M, Sanchez-Madrid F, Bustelo XR: F-actin-dependent translocation of the Rap1 GDP/GTP exchange factor RasGRP2. J Biol Chem 279, 20435–20446 (2004)
15. Ghandour H, Cullere X, Alvarez A, Luscinskas FW, Mayadas TN: Essential role for Rap1 GTPase and its guanine exchange factor CalDAG-GEFI in LFA-1 but not VLA-4 integrin mediated human T-cell adhesion. Blood 110, 3682–3690 (2007)
16. Czikora A, Lundberg DJ, Abramovitz A, Lewin NE, Kedei N, Peach ML, Zhou X, Merritt RC, Jr., Craft EA, Braun DC, Blumberg PM: Structural basis for the failure of the C1 domain of ras guanine nucleotide releasing protein 2 (RasGRP2) to bind phorbol ester with high affinity. J Biol Chem 291, 11133– 11147 (2016)
17. Fontenot JD, Gavin MA, Rudensky AY: Foxp3 programs the development and function of $CD4^+CD25^+$ regulatory T cells. Nat Immunol 4, 330–336 (2003)
18. Gambineri E, Torgerson TR, Ochs HD: Immune dysregulation, polyendocrinopathy, enteropathy, and X-linked inheritance (IPEX), a syndrome of systemic autoimmunity caused by mutations of FOXP3, a critical regulator of T-cell homeostasis. Curr Opin Rheumatol 15, 430–435 (2003)
19. Hori S, Nomura T, Sakaguchi S: Control of regulatory T cell development by the transcription factor Foxp3. Science 299, 1057–1061 (2003)
20. Khattri R, Cox T, Yasayko SA, Ramsdell F: An essential role for Scurfin in $CD4^+CD25^+$ T regulatory cells. Nat Immunol 4, 337–342 (2003)
21. Sakaguchi S, Yamaguchi T, Nomura T, Ono M: Regulatory T cells and immune tolerance. Cell 133, 775–787 (2008)
22. Brunkow ME, Jeffery EW, Hjerrild KA, Paeper B, Clark LB, Yasayko SA, Wilkinson JE, Galas D, Ziegler SF, Ramsdell F: Disruption of a new forkhead/winged-helix protein, scurfin, results in the fatal lymphoproliferative disorder of the scurfy mouse. Nat Genet 27, 68–73 (2001)
23. Bennett CL, Christie J, Ramsdell F, Brunkow ME, Ferguson PJ, Whitesell L, Kelly TE, Saulsbury FT, Chance PF, Ochs HD: The immune dysregulation, polyendocrinopathy, enteropathy, X-linked syndrome (IPEX) is caused by mutations of FOXP3. Nat Genet 27, 20–21 (2001)
24. Zanin-Zhorov A, Ding Y, Kumari S, Attur M, Hippen KL, Brown M, Blazar BR, Abramson SB, Lafaille JJ, Dustin ML: Protein kinase C-theta mediates negative feedback on regulatory T cell function. Science 328, 372–376 (2010)
25. Gavin M, Rudensky A: Control of immune homeostasis by naturally arising regulatory $CD4^+$ T cells. Curr Opin Immunol 15, 690–696 (2003)
26. Hickman SP, Yang J, Thomas RM, Wells AD, Turka LA: Defective activation of protein kinase C and Ras-ERK pathways limits IL-2 production and proliferation by $CD4^+CD25^+$ regulatory T cells. J Immunol 177, 2186–2194 (2006)
27. Tsang JY, Camara NO, Eren E, Schneider H, Rudd C, Lombardi G, Lechler R: Altered proximal T cell receptor (TCR) signaling in human $CD4^+CD25^+$ regulatory T cells. J Leukoc Biol 80, 145–151 (2006)
28. Ran FA, Hsu PD, Wright J, Agarwala V, Scott DA, Zhang F: Genome engineering using the CRISPR-Cas9 system. Nat Protoc 8, 2281–2308 (2013)
29. Müller LUW, Milsom MD, Kim M-O, Schambach A, Schuesler T, Williams DA: Rapid lentiviral transduction preserves the engraftment potential of $fanca^{-/-}$ hematopoietic stem cells. Molecular Therapy 16, 1154–1160 (2008)
30. Hurley JH, Newton AC, Parker PJ, Blumberg PM, Nishizuka Y: Taxonomy and function of C1 protein kinase C homology domains. Protein Sci 6, 477–480 (1997)
31. Kazanietz MG: Novel "nonkinase" phorbol ester receptors: the C1 domain connection. Mol Pharmacol 61, 759–767 (2002)
32. Colon-Gonzalez F, Kazanietz MG: C1 domains exposed: from diacylglycerol binding to protein-protein interactions. Biochim Biophys Acta 1761, 827–837 (2006)
33. Irie K, Masuda A, Shindo M, Nakagawa Y, Ohigashi H: Tumor promoter binding of the protein kinase C C1 homology domain peptides of RasGRPs, chimaerins, and Unc13s. Bioorg Med Chem 12, 4575–4583 (2004)
34. McLeod SJ, Li AH, Lee RL, Burgess AE, Gold MR: The Rap GTPases regulate B cell migration toward the chemokine stromal cell-derived factor-1 (CXCL12): potential role

for Rap2 in promoting B cell migration. J Immunol 169, 1365–1371 (2002)
35. Lio CW, Hsieh CS: A two-step process for thymic regulatory T cell development. Immunity 28, 100–111 (2008)
36. Tai PW, Wu H, Gordon JA, Whitfield TW, Barutcu AR, van Wijnen AJ, Lian JB, Stein GS, Stein JL: Epigenetic landscape during osteoblastogenesis defines a differentiation-dependent Runx2 promoter region. Gene 550, 1–9 (2014)
37. Dillon TJ, Carey KD, Wetzel SA, Parker DC, Stork PJ: Regulation of the small GTPase Rap1 and extracellular signal-regulated kinases by the costimulatory molecule CTLA-4. Mol Cell Biol 25, 4117–4128 (2005)
38. Gavin MA, Clarke SR, Negrou E, Gallegos A, Rudensky A: Homeostasis and anergy of $CD4^+CD25^+$ suppressor T cells in vivo. Nat Immunol 3, 33–41. (2002)
39. Huang YJ, Haist V, Baumgartner W, Fohse L, Prinz I, Suerbaum S, Floess S, Huehn J: Induced and thymus-derived $Foxp3^+$ regulatory T cells share a common niche. Eur J Immunol 44, 460–468 (2014)
40. Yang BH, Hagemann S, Mamareli P, Lauer U, Hoffmann U, Beckstette M, Fohse L, Prinz I, Pezoldt J, Suerbaum S, Sparwasser T, Hamann A, Floess S, Huehn J, Lochner M: $Foxp3^+$ T cells expressing RORgammat represent a stable regulatory T-cell effector lineage with enhanced suppressive capacity during intestinal inflammation. Mucosal Immunol 9, 444–457 (2016)
41. Ebinu JO, Stang SL, Teixeira C, Bottorff DA, Hooton J, Blumberg PM, Barry M, Bleakley RC, Ostergaard HL, Stone JC: RasGRP links T-cell receptor signaling to Ras. Blood 95, 3199–3203 (2000)
42. Yamashita S, Mochizuki N, Ohba Y, Tobiume M, Okada Y, Sawa H, Nagashima K, Matsuda M: CalDAG-GEFIII activation of Ras, R-ras, and Rap1. J Biol Chem 275, 25488–25493 (2000)
43. Teixeira C, Stang SL, Zheng Y, Beswick NS, Stone JC: Integration of DAG signaling systems mediated by PKC-dependent phosphorylation of RasGRP3. Blood 102, 1414–1420 (2003)
44. Yang Y, Li L, Wong GW, Krilis SA, Madhusudhan MS, Sali A, Stevens RL: RasGRP4, a new mast cell-restricted Ras guanine nucleotide-releasing protein with calcium- and diacylglycerol-binding motifs. Identification of defective variants of this signaling protein in asthma, mastocytosis, and mast cell leukemia patients and demonstration of the importance of RasGRP4 in mast cell development and function. J Biol Chem 277, 25756–25774 (2002)
45. Johnson JE, Goulding RE, Ding Z, Partovi A, Anthony KV, Beaulieu N, Tazmini G, Cornell RB, Kay RJ: Differential membrane binding and diacylglycerol recognition by C1 domains of RasGRPs. Biochem J 406, 223– 236 (2007)
46. Cifuni SM, Wagner DD, Bergmeier W: CalDAG-GEFI and protein kinase C represent alternative pathways leading to activation of integrin alphaIIbbeta3 in platelets. Blood 112, 1696–1703 (2008)
47. Nolz JC, Nacusi LP, Segovis CM, Medeiros RB, Mitchell JS, Shimizu Y, Billadeau DD: The WAVE2 complex regulates T cell receptor signaling to integrins via Abl- and CrkL-C3G-mediated activation of Rap1. J Cell Biol 182, 1231–1244 (2008)
48. Ren J, Cook AA, Bergmeier W, Sondek J: A negative-feedback loop regulating ERK1/2 activation and mediated by RasGPR2 phosphorylation. Biochem Biophys Res Commun 474, 193–198 (2016)
49. Onishi Y, Fehervari Z, Yamaguchi T, Sakaguchi S: $Foxp3^+$ natural regulatory T cells preferentially form aggregates on dendritic cells in vitro and actively inhibit their maturation. Proc Natl Acad Sci U S A 105, 10113–10118 (2008)

Supplementary material

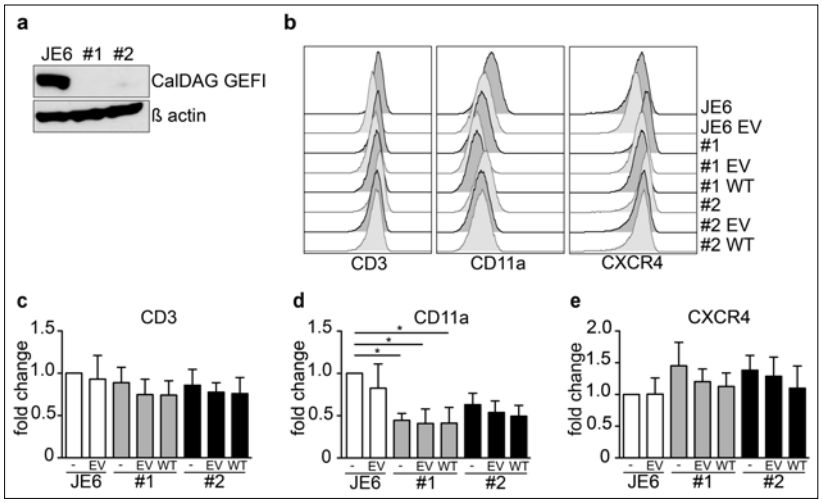

Suppl. Fig. 1. Characterization of CalDAG GEFI$^{-/-}$ Jurkat T cell clones. Two CalDAG GEFI$^{-/-}$ Jurkat T cell clones (no. 1 and no. 2) were generated via CRISPR-Cas9, and successful knock-out of CalDAG GEFI from JE6 Jurkat T cells was confirmed via (a) Western blot. β-Actin served as loading control. CalDAG GEFI$^{-/-}$ clones were characterized according to expression of CD3, CD11a, and CXCR4 as compared to wildtype JE6 Jurkat T cells via flow cytometry. To rescue expression alterations caused by CalDAG GEFI knock-out, both CalDAG GEFI$^{-/-}$ clones were reconstituted with wildtype CalDAG GEFI (WT) and transduction with empty vector backbone served as treatment control (EV). (b) Exemplary histogram overlays, pre-gated on living cells, for CD3, CD11a, and CXCR4 (left, middle, and right panel, respectively), show minor variations of the expression levels of the respective surface marker. Data are representative of five independently performed experiments. Surface expression of (c) CD3, (d) CD11a, and (e) CXCR4 was evaluated using the fold change of the Geomean of the respective marker gated on living cells. JE6, white bars; CalDAG GEFI$^{-/-}$ clone no. 1, grey bars, and no. 2, black bars; untransduced (−); empty vector transduced (EV) or CalDAG GEFI reexpressing (WT). Data were pooled from five independently performed experiments (mean ± SD)

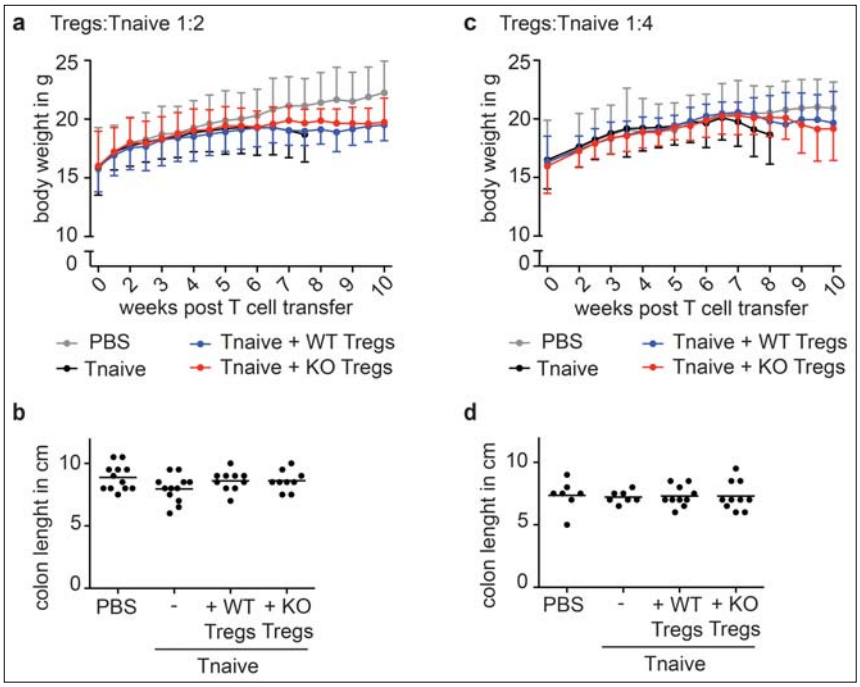

Suppl. Fig. 2. Suppressive capacity of CalDAG GEFI$^{-/-}$ Tregs in an *in vivo* model of transfer colitis. Capability of Tregs from CalDAG GEFI$^{+/+}$ and CalDAG GEFI$^{-/-}$ mice to suppress colon inflammation *in vivo* after cotransfer with Tnaive from CalDAG GEFI$^{+/+}$ into lymphopenic Rag2$^{-/-}$ mice was tested. PBS was injected as negative control (PBS). Rag2$^{-/-}$ mice were injected intra-peritoneally with Tnaive from CalDAG GEFI$^{+/+}$ mice only (no Tregs) or in combination with Tregs from either CalDAG GEFI$^{+/+}$ (WT Tregs) or CalDAG GEFI$^{-/-}$ (KO Tregs) mice at a ratio of (a, b) 1:2 or (c, d) 1:4 (Tregs: Tnaive). (a, c) Body weight of recipient mice (Tnaive, black curve; CalDAG GEFI$^{+/+}$ Tregs, WT, blue curve; CalDAG GEFI$^{-/-}$ Tregs, KO, red curve; PBS, grey curve) was monitored bi-weekly (mean ± SD), and mice were sacrificed at 80% of initial body weight or at the latest 10 weeks after cell transfer. (b, d) Colon length was monitored at the end of the experiment. Means of colon length within the indicated experimental groups are shown with each data point representing an individual mouse (pooled data from two to three independent experiments; n = 6– 12 mice per group)